TOP1 Mutations and Cross-Resistance to Antibody–Drug Conjugates in Patients with Metastatic Breast Cancer

Rachel O. Abelman[1], Bogang Wu[1], Haley Barnes[1], Arielle Medford[1], Bryanna Norden[1], Annika Putur[1], Elena Bitman[1], Win Thant[1], Ting Liu[1], Caroline Weipert[2], Geoffrey Fell[3], Laura M. Spring[1], Seth A. Wander[1], Beverly Moy[1], Neelima Vidula[1], Steven J. Isakoff[1], Andreas Varkaris[1], Dejan Juric[1], Ryan B. Corcoran[1], Leif W. Ellisen[1,4], and Aditya Bardia[1]

ABSTRACT

Purpose: Antibody–drug conjugates (ADC) harboring topoisomerase I (TOP1) inhibitor payloads have improved survival for patients with metastatic breast cancer. However, knowledge of ADC resistance mechanisms and potential impact on the sequential use of ADCs is limited. In this study, we report the incidence and characterization of *TOP1* mutations arising in the setting of ADC resistance in metastatic breast cancer.

Experimental Design: Patients with metastatic breast cancer treated with ADCs with available posttreatment plasma-based genotyping were included. *TOP1* mutation incidence, mutant allele frequency, and functional characterization were assessed, and incidence was compared with that in patients with metastatic breast cancer not receiving ADC treatment and in The Cancer Genome Atlas.

Results: Plasma-based genotyping identified distinct *TOP1* mutations (S57C, R364H, W401C, and G359E) in 12.9% of patients (4/31) at the time of disease progression on ADC, compared with 0.7% (3/420) in non–ADC-treated patients with metastatic breast cancer and 0.5% in The Cancer Genome Atlas. The appearance of mutations was associated with clinical cross-resistance, as median duration on the first ADC was 455 versus 52 days for the second ADC. The functional characterization of three novel TOP1-mutant proteins demonstrated that all exhibited reduced enzymatic activity, attenuated covalent DNA binding, and resistance to TOP1 inhibitor ADC payloads SN38 and deruxtecan.

Conclusions: We describe the recurrent emergence of functionally altered, resistance-associated *TOP1* mutations *in vivo* under selective pressure from ADCs and the potential impact on mediating cross-resistance to sequential ADCs. *TOP1* mutation may represent a biomarker of resistance in this setting, and additional work is needed to optimize biomarkers and ADC payload design to improve outcomes for the sequential use of ADCs.

See related commentary by Gwin and Hurvitz, p. 1824

Introduction

Antibody–drug conjugates (ADC) are innovative therapeutics designed to deliver highly potent chemotherapy directly to cells expressing tumor-associated antigens, allowing for efficient payload delivery while sparing normal tissues (1–3). These agents have been demonstrated to improve overall survival in patients with metastatic breast cancer (4). However, despite their general efficacy, patients typically experience disease progression within less than 1 year on treatment with ADCs and require a change in treatment. Although many patients are candidates for multiple ADCs and therefore receive sequential ADC treatment, retrospective data have demonstrated that patients experience shorter time on treatment with a second ADC. The specific molecular mechanisms driving this observation are not known (5–7). Previous work has demonstrated that the complex structure of ADCs provides many opportunities for resistance, including genetic alterations of the antigen target as well as the payload target, which we reported developing simultaneously in a single individual (8).

At present, two ADCs are approved by the FDA for use in HER2-low and HER2-negative metastatic breast cancer: trastuzumab deruxtecan (T-DXd) and sacituzumab govitecan (SG). T-DXd is targeted against the HER2 protein whereas SG is directed against TROP2, which are widely expressed in solid tumors (4, 9). Datopotamab deruxtecan, also targeting TROP2, has demonstrated promising results in hormone receptor–positive/HER2-negative metastatic breast cancer in the recent TROPION-Breast01 study (10). All three of these ADCs incorporate TOP1 inhibitors as their cytotoxic payloads. Topoisomerases, including topoisomerase I (TOP1), facilitate DNA replication and transcription by altering DNA topology, and they are well-established targets for antineoplastic therapy (11). TOP1 inhibitors such as camptothecin-based chemotherapies intercalate at the DNA/TOP1 interface to prevent the resolution of TOP1-induced single-strand breaks. The resulting stabilization of the so-called TOP1 cleavage complex (TOP1CC) ultimately leads to double-strand DNA breaks and subsequent cell death (11). Rapidly dividing cells, including malignant cells, are particularly sensitive to TOP1 inhibitors (11, 12). Under the selective pressure of high-dose TOP1 inhibitors *in vitro*, a variety of

[1]Massachusetts General Hospital, Harvard Medical School, Boston, Massachusetts. [2]Guardant Health, Inc., Palo Alto, California. [3]Dana Farber Cancer Institute, Harvard Medical School, Boston, Massachusetts. [4]Ludwig Center at Harvard, Boston, Massachusetts.

R.O. Abelman, B. Wu, and H. Barnes contributed equally to this article and share first authorship.

R.B. Corcoran, L.W. Ellisen, and A. Bardia contributed equally to this article and share senior authorship.

Corresponding Author: Leif W. Ellisen, MGH Cancer Center, CPZN-4204, 185 Cambridge Street, Boston, MA 02114. E-mail: lellisen@mgh.harvard.edu

Clin Cancer Res 2025;31:1966–74

doi: 10.1158/1078-0432.CCR-24-2771

Translational Relevance

Antibody–drug conjugates (ADC) targeting HER2 or trophoblast cell-surface antigen 2 (TROP2) and bearing topoisomerase I (TOP1) inhibitor cytotoxic payloads are now a mainstay for the treatment of all subtypes of metastatic breast cancer. However, the expression of HER2 and TROP2 is a poor predictor of ADC response, and there are no other clinically established biomarkers of response or resistance to these agents. Here, we report recurrent somatic mutations in *TOP1* in >10% of patients with metastatic breast cancer treated with TOP1 inhibitor–bearing ADCs. We demonstrate the association of these mutations with disease progression and with resistance to subsequent ADCs with TOP1 inhibitor payloads, and we provide direct evidence that they disrupt TOP1 function and confer TOP1 inhibitor resistance. These findings have near-term implications for *TOP1* mutation detection as a potential clinical diagnostic, particularly in the now-common clinical setting in which multiple TOP1 inhibitor ADCs are used sequentially. This work should also inform the optimal payload design for future ADCs.

TOP1 mutations have been described to emerge that confer drug resistance (11, 13, 14). However, such mutations seem to be exceedingly rare in the setting of acquired resistance to systemic TOP1 inhibitors *in vivo*.

With both of the approved ADCs for HER2-nonamplified metastatic breast cancer containing TOP1 inhibitor payloads, cross-resistance is a concern and could preclude their successful use in sequence. Retrospective clinical review has demonstrated that when patients receive sequential ADCs, the duration of response on their first ADC (ADC1) exposure is often substantially longer than the second ADC (ADC2; ref. 5). Multiple mechanisms may account for this observation, including alterations in target antigen expression, deregulated endolysosomal processing of the ADC, and payload efflux or alteration. Clinical evidence suggests that payload resistance may be particularly important, as higher response rates have been observed with a second ADC when an alternative payload was used (15, 16). Here, we report the emergence and characterization of *TOP1* mutations associated with treatment resistance in patients receiving sequential TOP1 inhibitor ADCs for metastatic breast cancer.

Materials and Methods

Patient cohorts and plasma-based tumor genotyping

Patients undergoing ctDNA testing using the GuardantOMNI assay performed for any tumor type as a part of usual clinical care at Massachusetts General Hospital (MGH) have results cataloged. This database was queried for all patients who had identified *TOP1* mutations found on ctDNA. This list was cross-referenced for all patients at MGH who received therapy for metastatic breast cancer. The cohort of "ADC patients" was defined as all patients treated with any ADC for metastatic breast cancer who had post-ADC ctDNA available within this database. The cohort of "patients with metastatic breast cancer" included all patients with metastatic breast cancer who had ctDNA testing available within this database. Testing for patients in these cohorts was performed between September 2020 and January 2024. All patients (or guardians) provided written informed consent under Institutional Review Board–approved protocols in accordance with the Declaration of Helsinki.

The GuardantOMNI platform was used for plasma-based genotyping/cell-free DNA (cfDNA) analysis. Testing was performed at Guardant Health, Inc., a Clinical Laboratory Improvement Amendments–certified, College of American Pathologists–accredited, and New York State Department of Health–approved laboratory. The 2.145 Mb GuardantOMNI assay identifies single-nucleotide variants and insertions and deletions in 496 genes, copy-number amplifications (106 genes), fusions (21 genes), microsatellite instability (MSI)-high status, and tumor mutational burden (17, 18). The validation of plasma tumor mutational burden and MSI has been previously described (19, 20). The Research Resource Identifier (RRID) for The Cancer Genome Atlas is SCR_003193.

Mutation quantitation

Whole blood was collected by routine phlebotomy in two 10-mL Streck tubes. Plasma was separated within 1 to 4 days of collection through two different centrifugation steps (the first at room temperature for 10 minutes at 1,600 × *g*, and the second at 3,000 × *g* for the same time and temperature). Plasma was stored at −80°C until cfDNA extraction.

Pretreatment tissue was collected at MGH in Boston, MA. The SNaPshot assay involves performing next-generation sequencing using anchored multiplex PCR, which identifies gene variants, rearrangements, insertions, and deletions (21). This assay was used to extract tissue nucleic acid that was amplified.

cfDNA was extracted from the stored plasma using QIAamp Circulating Nucleic Acid Kit (QIAGEN) with a 60-minute proteinase K incubation period at 60°C. All other steps were performed as described in the manufacturer's instructions.

Digital droplet PCR (ddPCR) analysis for mutation quantification was performed using a DNA template (up to 10 μL and 20 ng per specimen) along with 10 μL ddPCR Supermix for Probes (Bio-Rad) and 2 μL custom primer/probe mixture. The combination was integrated with a DG8 cartridge and 60 μL Droplet Generation Oil for Probes (Bio-Rad) to generate droplets, which were then moved to a 96-well plate (Eppendorf). Thermal cycling was performed under the following conditions: 10 minutes at 95°C, 40 cycles at 94°C for 30 seconds, 55°C (with a few grades of difference among assays) for 1 minute, and then 98°C for 10 minutes (ramp rate 2°C/second). The QX200 Droplet Reader (Bio-Rad) was used for droplet analysis and for fluorescent measurement of FAM and HEX probes. Positive and negative controls were used for the gating and identification of mutant populations. The QuantaSoft analysis software was used for data analysis and to calculate a mutant allele frequency (MAF). The quantification of the target molecule is described as the total copy number [mutant and wild-type (WT)] per sample. The MAF was calculated as follows: MAF% = [Nmut/(Nmut + Nwt) × 100], in which Nmut is the number of mutant alleles and Nwt is the number of WT alleles. Reference tumor mutations were selected by prevalence or previously known association with malignancy. Normal control human gDNA and no DNA template controls were always included. Probe and primer sequences are available upon request.

Cell lines and reagents

All cell lines were obtained from the ATCC and the MGH Center for Molecular Therapeutics cell bank. Cells underwent high-density SNP typing for identity authentication and were verified to be

Mycoplasma-free using MycoBlue Mycoplasma Detector (Vazyme, D101-01). All experiments shown were performed within a passage of <6 months from the acquisition of all cell lines. Cells were cultured at 37°C at 5% CO_2 in RPMI 1640 medium (Corning, 10-041-CV) containing 1% penicillin–streptomycin (Thermo Fisher Scientific, 15140122) and 10% FBS (Gibco, 26140079). TOP1 knockout (KO) virus was generated as previously mentioned using the TOP1 single-guide RNA CRISPR/Cas9 All-in-One Lentivector (Applied Biological Materials, 47302111). FLAG-tagged TOP1 carrying silent mutation for genomic DNA–targeting sequence and lentiviral vectors carrying red fluorescent protein (GeneUniversal) were transfected into HEK293T cells (RRID: CVCL_0063) with LV-MAX Lentiviral Packaging Mix (Thermo Fisher Scientific, A4237) using Lipofectamine 3000 Transfection Reagent protocol (Invitrogen, L3000031). After 48 hours, virus-containing media were collected and filtered using a 0.45-μmol/L pore filter (Millipore, SLHVR33RS). Parental or TOP1 KO HCC1806 (RRID: CVCL_1258) cells were transduced using filtered viral media with 8 μg/mL Polybrene (Sigma, TR-1003). Viral media were removed 24 hours later. The infected cells were collected, resuspended in 2% FBS in Dulbecco's PBS (Gibco, 14190250), and sorted by FACS based on red fluorescent protein expression levels. TOP1-mutant KO cell lines were then selected using puromycin (1 μg/mL) for 5 days.

Immunoprecipitation and Western blotting

Immunoprecipitation (IP) was performed using Pierce Magnetic IP Kit (Thermo Fisher Scientific, 88804). Briefly, cells were lysed in IP lysis buffer with protease/phosphatase inhibitor cocktail (Cell Signaling Technology, 5872) for 30 minutes. The lysates were sonicated and centrifuged at 13,000 × *g* to remove debris. The lysates were incubated overnight with FLAG antibody (Invitrogen, MA1-91878, RRID: AB_1957945) and beads. The eluates were pH-neutralized and stored for Western blot confirmation and further experiments. For whole-cell lysates, cultured cells were lysed with 1× SDS lysis buffer (GenScript, MB01015) and were subjected to standard SDS-PAGE. The primary antibodies included anti-FLAG (Cell Signaling Technology, 8146, RRID: AB_10950495), anti-TOP1 (Abcam, 109374, RRID: AB_10861978), and anti–B-actin (Cell Signaling Technology, 3700, RRID: AB_2242334).

DNA relaxation assay

Immunoprecipitated TOP1 protein functional activity was assessed using Human Topoisomerase I Assay Kit (TopoGEN, TG1015) according to the manufacturer's protocol. The reaction mixture (20 μL) included 0.25 ng of pHOT1 DNA and indicated volumes of TOP1 WT and mutant extracts mixed in the reaction buffer (10 mmol/L Tris-HCl, pH 7.9, 1 mmol/L EDTA, 0.15 mol/L NaCI, 0.1% BSA, 0.1 mmol/L spermidine, and 5% glycerol). The reaction mixtures were prepared on ice. After 30 minutes of incubation at 37°C, the reaction was terminated by the addition of the stop buffer (0.125% bromophenol blue, 25% glycerol, and 5% sarkosyl). The samples were then subjected to 1% agarose gel electrophoresis, stained with 1× GelRed, and visualized on ChemiDoc (Bio-Rad). Quantifications were performed using ImageJ (RRID: SCR_003070).

Proliferation and drug sensitivity assays

Cells were seeded in a 96-well plate (2,000–3,000 cells per well) and allowed to attach overnight. The following day, the cells were treated with the indicated doses of SN38 (Tocris, 2684) and maintained under physiologic conditions. Cells were imaged every 6 hours using the Incucyte S3 Live-Cell Analysis System (Sartorius). Viable cell proliferation graphs were generated using the Incucyte image analysis software from 10X phase images. Percent well confluency values were normalized to control wells to calculate relative cell numbers. Relative cell numbers were normalized to WT before reaching confluency and graphed in GraphPad Prism 8 (GraphPad Software Inc., RRID: SCR_002798). After 3 to 4 days, cell viability was assessed using CellTiter-Glo assay (Promega, G9241) according to the manufacturer's protocol.

TOP1 DNA-binding assay

The detection of DNA-bound TOP1 was performed according to the published protocol with minor modifications (22). Cells (0.6 million) were seeded in a 60-mm dish and allowed to attach overnight. The next day, cells were treated with 0.25 μmol/L SN38 for 15 minutes. The media were quickly aspirated, and the cells were lysed with DNAzol (Invitrogen, 10503027). Cells were collected by scraping and transferred into an Eppendorf tube. Cold 100% ethanol was added to precipitate the DNA. Samples were vortexed briefly and incubated at −20°C for 10 minutes. The DNA was pelleted at 10,000 rpm for 10 minutes at 4°C. After removing the supernatant, the DNA pellet was washed twice with cold 70% ethanol and then resuspended in 8 mmol/L NaOH. Concentrations were quantified using NanoDrop and then normalized. The samples were then loaded into a dot blot apparatus and then probed using anti-FLAG (Cell Signaling Technology, 8146, RRID: AB_10950495), anti-TOP1 (Abcam, 109374, RRID: AB_10861978), and anti-dsDNA (Abcam, 27156, RRID: AB_470907) antibodies.

γ-H2AX assessment by flow cytometry

The detection of γ-H2AX foci was performed using eBioscience Foxp3/Transcription Factor Staining Buffer Set (Invitrogen, 00-5523-00) and assessed via flow cytometry. Cells (0.05 million) were seeded in a 12-well plate and allowed to attach overnight. The next day, cells were treated with 0.8 nmol/L SN38 for 24 hours. Cells were trypsinized, washed with PBS, and then underwent staining as per the manufacturer's intracellular staining protocol with minor modifications. After fixation and permeabilization, the samples were blocked using 2% FBS for 15 minutes at room temperature. Samples were then stained with Anti–phospho Histone H2A.X Alexa Fluor 488 Conjugate Antibody (MilliporeSigma, 6A2770, RRID: AB_309864) for 30 minutes at room temperature. After washing, the samples were stained with 4',6-diamidino-2-phenylindole (Sigma, 10236276001, RRID: AB_2629482) at 1 μg/mL and immediately subjected to flow cytometry. Data were analyzed using FlowJo v10.8 Software (BD Life Sciences, RRID: SCR_008520).

Data availability

Deidentified patient data reported in the article may be requested from the corresponding authors and will be available for up to 6 years after publication. The release of deidentified data involves a formal review process that includes ensuring that any transfer is in compliance with the Institutional Review Board. The requesting investigator will be required to sign a data release form prior to transfer. Raw data supporting the figures and graphs as well as full blots are available from the authors upon request.

Results

Frequency of TOP1 mutations

To understand the incidence of *TOP1* mutations in patients who have received ADCs for metastatic breast cancer, we identified all

Table 1. Baseline characteristics of ADC patients with and without *TOP1* mutations.

Characteristics	ADC patients with *TOP1* mutations (*n*, %), total *n* = 4	ADC patients without *TOP1* mutations (*n*, %), total *n* = 27
Age (median)	54.9 years	63.4 years
Age 50		
≤50	1 (25%)	6 (22.2%)
>50	3 (75%)	21 (77.8%)
Sex		
Female	4 (100%)	27 (100%)
Race		
White	4 (100%)	20 (74.1%)
Asian		2 (7.4%)
Black		1 (3.7%)
Unknown		4 (14.8%)
Ethnicity		
Ethnicity not known	1 (25%)	1 (3.7%)
Non-Hispanic	3 (75%)	24 (88.9%)
Hispanic		2 (7.4%)
ECOG PS		
0	2 (50%)	11 (40.7%)
1	2 (50%)	12 (44.4%)
2		2 (7.4%)
n/a		2 (7.4%)
Time from metastatic diagnosis to the start of ADC1 (median) days	605.5 days	637 days
Previous total metastatic treatment lines (median)	3.5	2
Previous treatment		
Chemotherapy	4 (100%)	21 (77.8%)
Endocrine therapy	2 (50%)	14 (51.9%)
Targeted therapy	3 (75%)	18 (66.7%)

Abbreviation: ECOG PS, Eastern Cooperative Oncology Group performance status; n/a, not applicable.

patients at our institution who had undergone plasma-based ctDNA analysis (500-gene GuardantOMNI panel) before and after disease progression on an ADC ($N = 31$). The baseline characteristics of the patients are outlined in **Table 1**. Of 31 patients identified to have pre/post-progression ctDNA analysis, 4 (12.9%) were found to have *TOP1* mutations (**Fig. 1A**). This mutation prevalence compares with a 0.7% frequency of *TOP1* mutation among a cohort of 420 patients with metastatic breast cancer who had not received an ADC and a 0.5% frequency in primary breast cancer in The Cancer Genome Atlas, highlighting a higher frequency in the metastatic breast cancer setting after exposure to ADCs with TOP1 inhibitor payloads (**Fig. 1A**). In each case, a unique missense *TOP1* mutation was identified: R364H, S57C, G359E, and W401C (**Fig. 1B**). $TOP1^{R364H}$ has been previously reported as a *bona fide* camptothecin resistance–inducing mutation arising *in vitro* (23), whereas the other mutations have not been previously reported. All mutations except $TOP1^{S57C}$ were found exclusively in association with disease progression. Although numbers are small, no substantial differences in clinical characteristics were apparent between patients in this cohort who did versus did not develop *TOP1* mutations (**Table 1**).

Clinical outcomes and the emergence of mutations with sequential ADCs

We evaluated the clinical outcomes of sequential ADC exposure in patients with *TOP1*-mutant metastatic breast cancer. All four patients derived clinical benefit from ADC1 but had limited benefit from ADC2. MGH1 and MGH4 experienced essentially *de novo* progression (within <60 days) on ADC2, and MGH2 was found to have progressive disease at first-interval restaging (**Fig. 1B** and **C**). In all but one case (MGH3), both ADCs contained TOP1 inhibitor payloads. Overall, the median duration on ADC1 was 455 days, whereas the median duration on ADC2 was 52 days, excluding patient MGH3 who stopped after one cycle because of toxicity.

To evaluate the temporal emergence of *TOP1* mutations, we designed mutation-specific assays and carried out ddPCR analysis of isolated DNA from patient serial blood and tissue samples to quantitate the prevalence of each mutation in relation to treatment with sequential ADCs (**Fig. 1C**). In parallel, we assessed the prevalence of additional patient-specific tumor-associated mutations detected in the pre-ADC samples. No *TOP1* mutations were detectable before the start of ADC1 in three of four patients despite the detection of other tumor mutations. However, serial DNA specimens revealed the emergence or increased frequency of *TOP1* mutations after the initiation of therapy with ADC1 in each case. Notably, in multiple cases, *TOP1* mutations emerged even as the MAF of other tumor mutations declined, potentially suggesting the growth of a resistant tumor subclone. The *TOP1* MAF further increased after treatment with a second TOP1 inhibitor ADC in two cases (MGH1 and MGH2) and correlated with the lack of therapeutic response. MGH2 was found to have a low-level *TOP1* mutation prior to the initiation of ADC treatment but nonetheless remained on ADC1 therapy for 13 months. The MAF for S57C increased slightly after treatment with ADC1 (1.06%–2.21%)

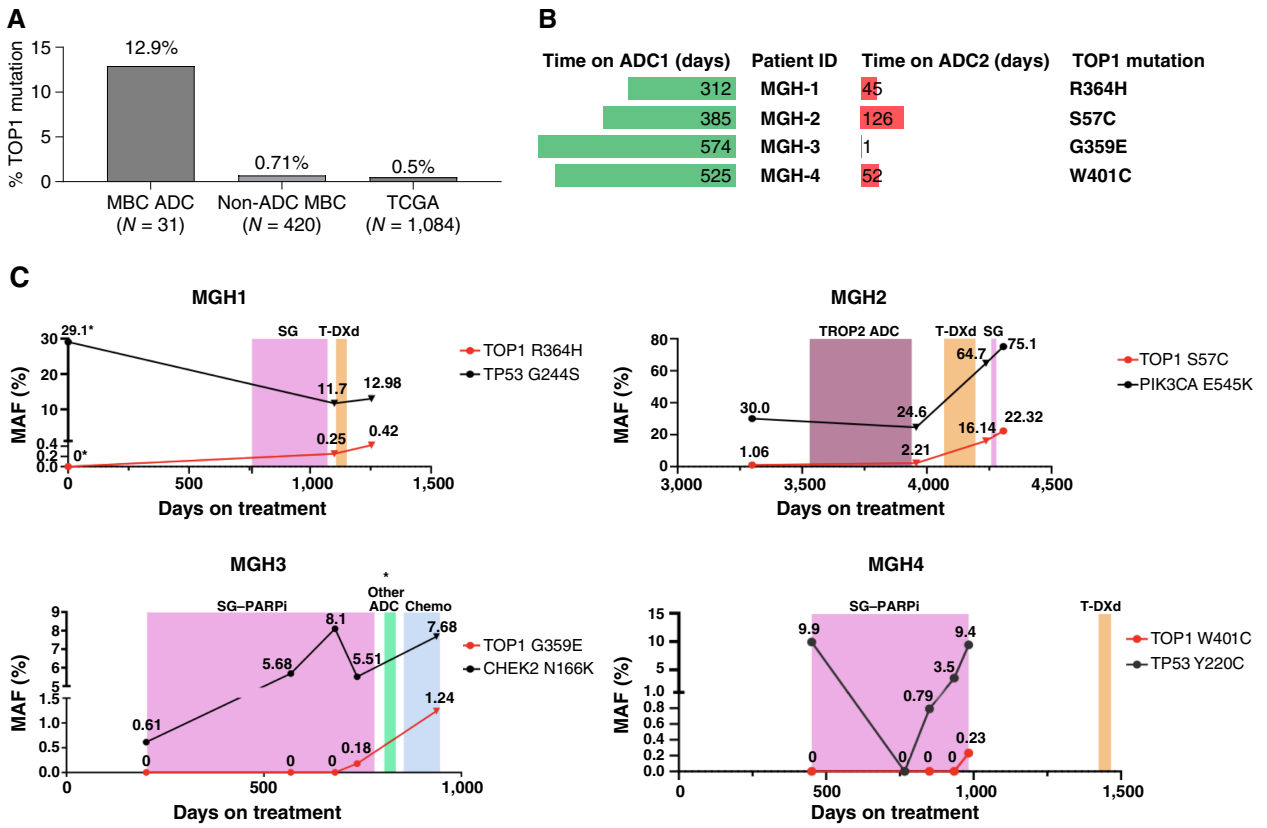

Figure 1.

Prevalence, clinical course, and quantitation associated with *TOP1* somatic mutations. **A,** *TOP1* mutation percentages associated with (i) MBC after ADC therapy, (ii) MBC and no prior ADC therapy, and (iii) primary tumors in the TCGA database. **B,** Summary of time on treatment for four patients in the MGH cohort who received sequential ADCs for MBC, including time on ADC1, time on ADC2, and the identity of the *TOP1* mutation. **C,** Clinical course and MAF assessed in plasma for four patients with TOP1 mutations. Day 0 is the day of diagnosis of MBC. Time on treatment with each ADC is outlined in color. The MAF of each *TOP1* mutation and a reference mutation identified in each patient is indicated on the *Y*-axis. Samples represented with circles are values from ddPCR data, whereas those represented by triangles reflect values from GuardantOMNI testing. All samples represent GuardantOMNI samples except the first timepoint of MGH1, which was a tumor (asterisk). MGH3 received a non-TOP1 inhibitor ADC for ADC2 (asterisk). Chemo, chemotherapy; MBC, metastatic breast cancer; PARPi, PARP inhibitor; TCGA, The Cancer Genome Atlas.

but more meaningfully after treatment with ADC2 (from 2.21% to 22.32%), reflecting the increase in refractory disease burden despite therapy (**Fig. 1C**). Further clinical details of the individual cases are included in Supplementary Table S1.

Functional characterization of individual TOP1-mutant proteins

The mutations of *TOP1* are an established mechanism of resistance to TOP1 inhibitors, but almost all previously described mutations have been observed only in cells exposed to TOP1 inhibitors *in vitro* (24). As noted, TOP1 inhibitors function by intercalating between TOP1 and DNA, resulting in stabilization of the TOP1CC and ultimately giving rise to double-strand DNA breaks and cell death (25). Most resistance-associated missense mutations in human *TOP1* have been found in the core domain (residues 214–635) and are thought to alter TOP1 structure and enzymatic activity (26). Indeed, three of four mutations we identified were located within the core domain, and all four mutations occurred at conserved amino acid residues (**Fig. 2A** and **B**). As noted, R364H was previously observed to arise *in vitro* in a camptothecin-resistant tumor cell line and has been characterized in detail (23), whereas the other three mutations have not been previously reported. Accordingly, we sought to test the enzymatic activity of these three novel mutant proteins and to determine whether they were indeed associated with resistance to the ADC TOP1 inhibitor payloads.

We first purified WT and mutant TOP1 proteins S57C, G359E, and W401C by expressing each *in vitro* followed by IP via the epitope tag (**Fig. 3A**). We then carried out a relaxation assay whereby an equal amount of each protein is incubated with supercoiled DNA followed by gel electrophoresis. Consistently, both G359E and W401C demonstrated <50% of WT activity in this assay, whereas the activity of S57C was also reduced but to a lesser degree (**Fig. 3B** and **C**). We next tested the ability of these mutant proteins to confer resistance to TOP1 inhibitor payloads in triple negative breast cancer (TNBC) cells. Interestingly, tumor cells exhibited variable tolerance to the expression of the different mutants even in cells expressing endogenous TOP1, with the lowest expression being observed for W401C (**Fig. 3D**). Nevertheless, in each case, quantitative dose–response analysis demonstrated that cells expressing each of the three mutants were more resistant to both ADC payloads SN38 (for SG) and

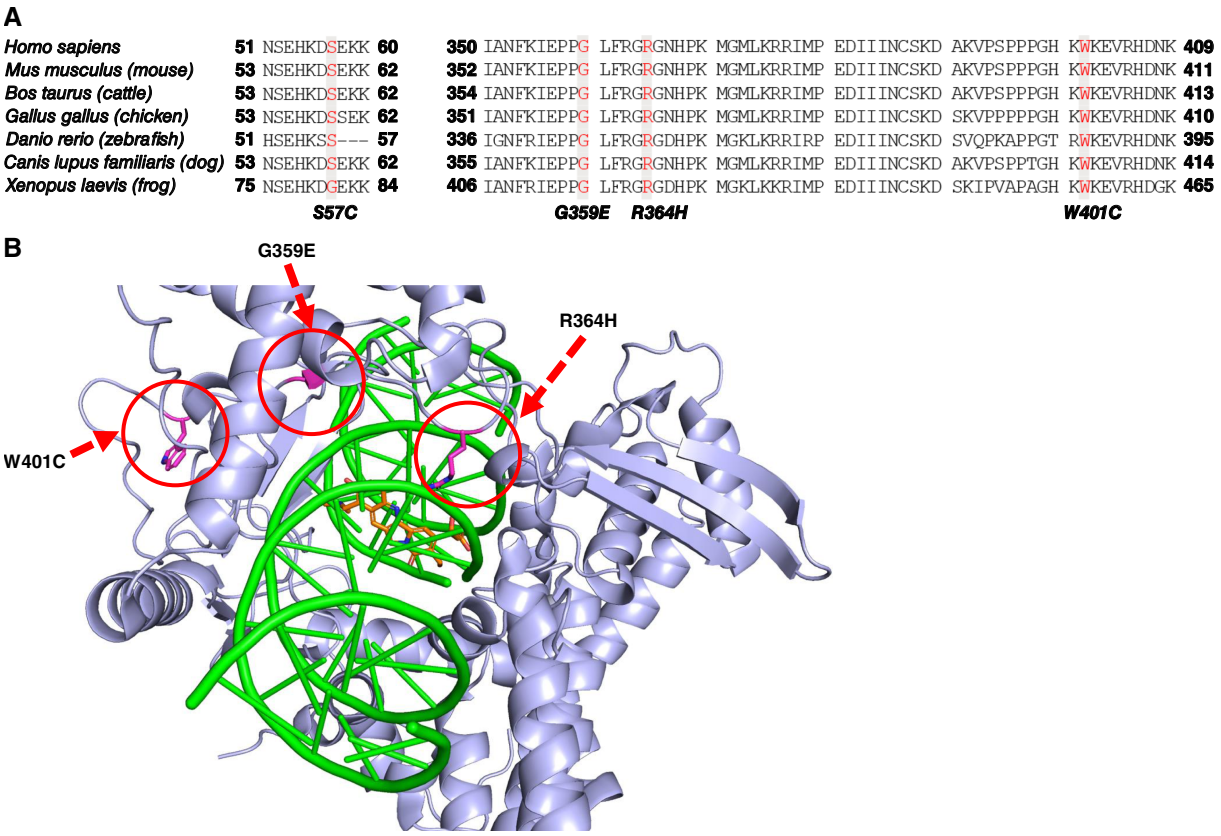

Figure 2.

Location and conservation of identified TOP1-mutant amino acids. **A,** Alignment of TOP1 amino acid sequence regions harboring identified mutations. Mutation-associated amino acids across species are indicated in red, and alterations are shown below. **B,** Schematic crystal structure of DNA-bound human TOP1 protein/inhibitor (topotecan) complex. Mutated amino acid residues (purple) are highlighted by red circles, and topotecan is shown in orange. The three mutations within TOP1 core domain (residues 214–635) are highlighted. S57C, which is located within an unstructured NH2-terminal domain, is not shown.

deruxtecan (for T-DXd) than cells expressing ectopic WT TOP1, and this was particularly notable at lower TOP1 inhibitor doses (**Fig. 3E**; Supplementary Fig. S1A and S1B). Notably, expression of the mutant proteins did not significantly impede proliferation of the cells (Supplementary Fig. S1B and S1C). Furthermore, TOP1 inhibitor resistance was associated with statistically significantly decreased DNA damage following SN38 treatment in cells expressing each of the mutants compared with that in WT TOP1, as assessed by γ-H2AX staining. This was particularly the case for G359E which was the most highly expressed of the mutants (Supplementary Fig. S1D and S1E).

Given that *TOP1* mutation–associated inhibitor resistance has been linked to the altered binding of inhibitor to the mutant complex, we next carried out quantitative binding assessment in cells expressing each mutant protein (27). We first generated pools depleted of endogenous TOP1 with CRISPR/Cas9 engineering. We then treated cells with SN38 to stabilize TOP1 covalently bound to DNA, followed by chromatin purification and quantitation of DNA-bound TOP1 using an established protocol (28). TOP1CC formation was decreased in mutant-expressing cells, with G359E in particular showing a substantial decrease in TOP1CC incorporation (**Fig. 3F**; Supplementary Fig. S1F). Taken together, these results demonstrate that all the mutations we identified in patients exhibiting TOP1 inhibitor–associated ADC resistance disrupt TOP1 function and confer resistance to TOP1 inhibitors.

Discussion

Here, we report the emergence of unique *TOP1* mutations associated with clinical progression and cross-resistance to multiple ADCs delivering TOP1 inhibitor payloads in patients with metastatic breast cancer. Several lines of evidence point to the clinical relevance of these *TOP1* mutations for ADC resistance and cross-resistance. First, all the mutations except one were not detected in the pre-ADC samples, and all four increased substantially at the time of clinical progression. Second, all four missense *TOP1* mutations involved conserved amino acids, whereas three of the four mutations identified were within the core domain, in which many *bona fide* TOP1 resistance–inducing mutations are localized. This includes the previously identified *TOP1* mutation, R364H, reported to arise *in vitro* under drug selection within a camptothecin-resistant cell line. Third, although we found the three novel mutant proteins to be variably defective in enzymatic activity, with S57C activity being closest to WT, each mutant protein is indeed sufficient to confer resistance to the SG payload SN38 when expressed in TNBC cells. In each case, resistance was associated with decreased DNA damage in cells expressing the mutants compared with WT

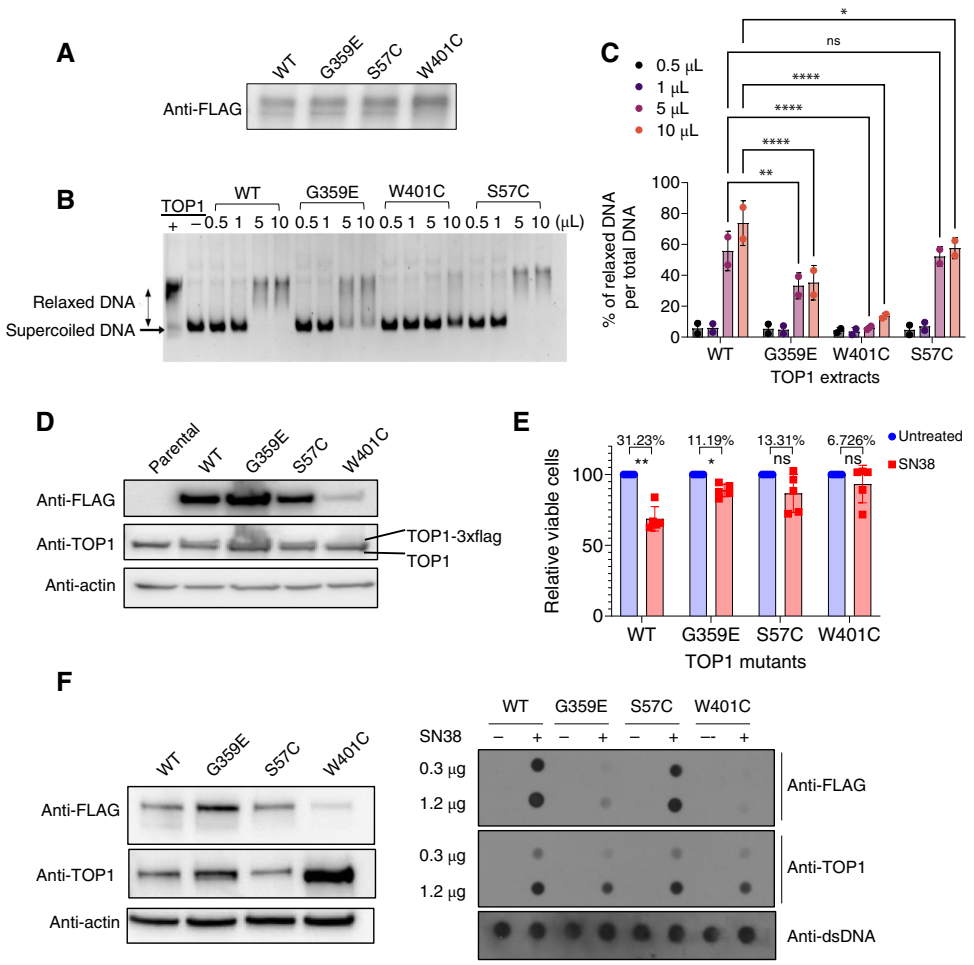

Figure 3.
Altered enzymatic activity, DNA binding, and TOP1 inhibitor resistance of TOP1-mutant proteins. **A,** IP–Western blot of Flag-tagged TOP1 after anti-FLAG IP from CRISPR/Cas9-TOP1 HCC1806 cells reconstituted with WT or mutant TOP1. **B,** TOP1-mediated plasmid relaxation. Supercoiled pHOT1 plasmid was incubated for 30 minutes with the indicated amount of TOP1-Flag IP extracts. **C,** Quantification of percent relaxed DNA from **B**, $n = 3$ experimental repeats. *, $P < 0.05$; **, $P < 0.01$; ****, $P < 0.0001$. P values were calculated by two-way ANOVA followed by a multiple comparison test (Fisher LSD test). **D,** Western blots of Flag-tagged ectopic TOP1 and total TOP1 in parental HCC1806 TNBC cells. **E,** Summary of dose–response analysis following SN38 treatment (0.18–0.8 nmol/L, 3 days) of cells from **D**, $n = 5$ experimental repeats. P values were calculated by multiple unpaired t tests. **F,** Western blots of Flag-tagged ectopic TOP1 and total TOP1 in CRISPR/Cas9-TOP1 HCC1806 cell pools (left side). Dot blots showing G359E and W401C exhibit the most reduction of SN38-stabilized TOP1 DNA binding, as assessed by the RADAR assay (right side; see "Materials and Methods"). dsDNA, double-strand DNA; ns, nonsignificant.

TOP1. Although further detailed studies will be required to fully vet the contribution of each of these mutants to TOP1 inhibitor resistance, these results are in keeping with our previous report of an acquired *TOP1* mutation, E418K, in multiple sites of metastasis in a patient with disease progression on SG (8). Like *TOP1*^{R364H}, E418K has been previously identified *in vitro* in the setting of induced TOP1 inhibitor resistance. These two mutations have been shown experimentally and by molecular modeling to decrease inhibitor binding to the mutant complex (29). Notably, in the case of the patient whose diseases harbored E418K, we found that distinct metastatic lesions showed a novel acquired resistance–inducing missense mutation in *TACSTD2/TROP2*, highlighting the potential for both target- and payload-directed resistance mutations to ADCs.

The prevalence of *TOP1* mutations as a resistance mechanism to ADCs in metastatic breast cancer was previously unknown, but in this cohort, it was found to be 12.9%, compared with <1% in patients with metastatic breast cancer not treated with ADCs. Although larger studies will be needed to further elucidate the prevalence of such mutations, our data suggest that they are a highly relevant and recurrent occurrence, with broad clinical implications for ADC selection and therapeutic sequencing. In addition, our findings are unlikely to be restricted to patients with breast cancer, as a recent report describes a patient with advanced non–small cell lung cancer treated with the HER3-directed ADC patritumab deruxtecan (also with a TOP1 inhibitor payload) who developed a *TOP1*^{L721R} mutation in the setting of acquired resistance (30). Undoubtedly, the relevance of *TOP1* mutations as a resistance mechanism will increase as more patients are treated with these agents and the number of TOP1 inhibitor–associated ADCs in clinical development continues to grow.

The relatively common occurrence of *TOP1* mutations associated with resistance to ADCs suggests several strategies to limit cross-resistance. For example, identifying patients with such payload (and/or antibody target) mutations at the time of progression on an initial ADC would allow for the selection of an optimal subsequent ADC candidate to maximize efficacy. Our demonstration that these mutations are detectable through clinically available blood-based analysis implies that this strategy could be used relatively quickly for clinical decision making. As our findings suggest that these mutations confer resistance to payloads of multiple currently approved ADCs, the subsequent use of ADCs bearing alternative classes of payloads would be a logical choice. In addition, TOP1 inhibitors remain attractive as payloads, and the literature suggests the existence of alternative TOP1 inhibitors that may be refractory to such *TOP1* mutations and that could theoretically be incorporated into ADCs for sequential therapy (31). Nonetheless, our findings would seem to warrant caution against overreliance on this class of drugs and hopefully will encourage

the development of future ADCs incorporating a diversity of cytotoxic and bioactive payloads.

In summary, *TOP1* mutations are rare prior to treatment but repeatedly emerge in association with disease progression and resistance in patients with metastatic breast cancer treated with ADCs containing TOP1 inhibitor payloads. These mutations are readily detectable and likely to mediate cross-resistance to the sequential use of existing ADCs with TOP1 inhibitor payloads. Thus, this study demonstrates the need to establish these mutations as bona fide clinical diagnostics and to optimize rational sequencing and the future development of ADCs that overcome *TOP1* mutation–associated clinical resistance.

Authors' Disclosures

R.O. Abelman reports a grant from the Conquer Cancer Foundation during the conduct of the study. B. Wu reports a grant from the Terri Brodeur Breast Cancer Foundation during the conduct of the study. A. Medford reports personal fees from AstraZeneca, Edgewood Oncology, Guardant Health, Illumina, Myriad Genetics, Natera, and Science for America and a grant from the National Institutes of Health (K12) outside the submitted work. C. Weipert is an employee and a stockholder of Guardant Health, Inc. L.M. Spring reports service as a consultant/service on the advisory board of Novartis, Daiichi Pharma, AstraZeneca, Eli Lilly, Precede, and Seagen; institutional research support from Merck, Genentech, Gilead, Eli Lilly, and AstraZeneca; and travel support from Eli Lilly. S.A. Wander reports personal fees from Foundation Medicine, Veracyte, Hologic, Biovica, Novartis, and AstraZeneca; personal fees and other support from Eli Lilly, Pfizer/Arvinas, Puma Biotechnology, Genentech, Regor Therapeutics, and Stemline/Menarini; and other support from Sermonix, Guardant Health, and 2ndMD outside the submitted work. N. Vidula reports grants from Merck, Radius, Daehwa, Novartis, Pfizer, and Stemline and personal fees from Gilead, Aadi, TerSera, Novartis, and IDEOlogy Health outside the submitted work. D. Juric reports grants and personal fees from Novartis, Genentech, Syros, Eisai, Pfizer, and Takeda; personal fees from Vibliome, PIC Therapeutics, Mapkure, and Relay Therapeutics; and grants from Amgen, InventisBio, Arvinas, Blueprint, AstraZeneca, Ribon Therapeutics, and Scorpion Therapeutics outside the submitted work. R.B. Corcoran reports personal fees and other support from Sidewinder Therapeutics, Alterome Therapeutics, Pheon Therapeutics, C4 Therapeutics, Cogent Biosciences, Erasca, Kinnate Biopharma, Nested Therapeutics, nRichDx, Remix Therapeutics, and Revolution Medicines; personal fees from AbbVie, Amgen, Bristol Myers Squibb, Elicio, Parabilis Medicines, Genentech/Roche, Mirati Therapeutics, Qiagen, and Taiho; and grants from Invitae, Novartis, Relay Therapeutics, and OnKure outside the submitted work. L.W. Ellisen reports a grant from National Institutes of Health (R01) and the Congressionally Directed Medical Research Programs (CDMRP) during the conduct of the study as well as personal fees from Gilead, AstraZeneca, Atavistik, and Kisoji and other support from Sanofi outside the submitted work; in addition, L.W. Ellisen reports a patent for PCT/US2022/079958 pending. A. Bardia reports a grant from National Institutes of Health (R01) and the CDMRP and grants and personal fees from Pfizer, Novartis, Genentech, Merck, Menarini, Gilead, Sanofi, AstraZeneca, Daiichi Sankyo, and Eli Lilly during the conduct of the study, as well as a patent for Trop 2 ADC and PARPi pending. No disclosures were reported by the other authors.

Authors' Contributions

R.O. Abelman: Conceptualization, data curation, investigation, writing–original draft, writing–review and editing. **B. Wu:** Data curation, formal analysis, supervision, investigation, methodology. **H. Barnes:** Data curation, investigation, methodology, writing–review and editing. **A. Medford:** Conceptualization, investigation, writing–review and editing. **B. Norden:** Data curation, investigation, methodology, writing–review and editing. **A. Putur:** Data curation, writing–review and editing. **E. Bitman:** Data curation, investigation, methodology. **W. Thant:** Data curation, investigation. **T. Liu:** Data curation, writing–review and editing. **C. Weipert:** Resources, writing–review and editing. **G. Fell:** Methodology, writing–review and editing. **L.M. Spring:** Conceptualization, writing–review and editing. **S.A Wander:** Writing–review and editing. **B. Moy:** Writing–review and editing. **N. Vidula:** Writing–review and editing. **S.J. Isakoff:** Writing–review and editing. **A. Varkaris:** Writing–review and editing. **D. Juric:** Writing–review and editing. **R.B. Corcoran:** Conceptualization, resources, supervision, funding acquisition, investigation, writing–original draft, writing–review and editing. **L.W. Ellisen:** Conceptualization, resources, supervision, funding acquisition, writing–original draft, writing–review and editing. **A. Bardia:** Conceptualization, resources, supervision, funding acquisition, investigation, writing–original draft, writing–review and editing.

Acknowledgments

This work was supported by Department of Defense/CDMRP grant BC200924 and by R01CA260890 (to L.W. Ellisen and A. Bardia), the Terri Brodeur Breast Cancer Foundation Fellowship, NIH/NCI K99CA286969 (to B. Wu), the American Society of Clinical Oncology Young Investigator Award (to R.O. Abelman), an NIH K12 grant K12CA087723 (to A. Medford), and the Tracey Davis Memorial Breast Cancer Research Fund. The authors thank Amanda Jung for her assistance with data curation.

Note

Supplementary data for this article are available at Clinical Cancer Research Online (http://clincancerres.aacrjournals.org/).

Received August 25, 2024; revised November 8, 2024; accepted December 30, 2024; posted first January 2, 2025.

References

1. Abelman RO, Wu B, Spring LM, Ellisen LW, Bardia A. Mechanisms of resistance to antibody-drug conjugates. Cancers (Basel) 2023;15:1278.
2. Shastry M, Gupta A, Chandarlapaty S, Young M, Powles T, Hamilton E. Rise of antibody-drug conjugates: the present and future. Am Soc Clin Oncol Educ Book 2023;43:e390094.
3. Chang HL, Schwettmann B, McArthur HL, Chan IS. Antibody-drug conjugates in breast cancer: overcoming resistance and boosting immune response. J Clin Invest 2023;133:e172156.
4. Bardia A, Hurvitz SA, Tolaney SM, Loirat D, Punie K, Oliveira M, et al. Sacituzumab govitecan in metastatic triple-negative breast cancer. N Engl J Med 2021;384:1529–41.
5. Abelman RO, Spring L, Fell GG, Ryan P, Vidula N, Medford AJ, et al. Sequential use of antibody-drug conjugate after antibody-drug conjugate for patients with metastatic breast cancer: ADC after ADC (A3) study. J Clin Oncol 2023;41(Suppl 16):1022.
6. Fenton MA, Tarantino P, Graff SL. Sequencing antibody drug conjugates in breast cancer: exploring future roles. Curr Oncol 2023;30:10211–23.
7. Huppert LA, Mahtani R, Fisch SC, Dempsey N, Premji S, Taylor A, et al. Multicenter retrospective cohort study of the sequential use of the antibody-drug conjugates (ADCs) trastuzumab deruxtecan (T-DXd) and sacituzumab govitecan (SG) in patients with HER2-low metastatic breast cancer (MBC): updated data and subgroup analyses by age, sites of disease, and use of intervening therapies. J Clin Oncol 2024;42(Suppl 16):1083.
8. Coates JT, Sun S, Leshchiner I, Thimmiah N, Martin EE, McLoughlin D, et al. Parallel genomic alterations of antigen and payload targets mediate polyclonal acquired clinical resistance to sacituzumab govitecan in triple-negative breast cancer. Cancer Discov 2021;11:2436–45.
9. Modi S, Saura C, Yamashita T, Park YH, Kim S-B, Tamura K, et al. Trastuzumab deruxtecan in previously treated HER2-positive breast cancer. N Engl J Med 2020;382:610–21.
10. Bardia A, Jhaveri K, Kalinsky K, Pernas S, Tsurutani J, Xu B, et al. TROPION-Breast01: datopotamab deruxtecan vs chemotherapy in pre-treated inoperable or metastatic HR+/HER2− breast cancer. Future Oncol 2024;20:423–36.
11. Thomas A, Pommier Y. Targeting topoisomerase I in the era of precision medicine. Clin Cancer Res 2019;25:6581–9.
12. Pommier Y, Thomas A. New life of topoisomerase I inhibitors as antibody-drug conjugate warheads. Clin Cancer Res 2023;29:991–3.

13. Saleem A, Ibrahim N, Patel M, Li XG, Gupta E, Mendoza J, et al. Mechanisms of resistance in a human cell line exposed to sequential topoisomerase poisoning. Cancer Res 1997;57:5100–6.
14. Chrencik JE, Staker BL, Burgin AB, Pourquier P, Pommier Y, Stewart L, et al. Mechanisms of camptothecin resistance by human topoisomerase I mutations. J Mol Biol 2004;339:773–84.
15. Chen M, Huang R, Chen R, Pan, F, Shen, X, Li, H, et al, Optimal sequential strategies for antibody-drug conjugate in metastatic breast cancer: evaluating efficacy and cross-resistance. Oncologist 2024;29:e957–66.
16. García-Alonso S, Ocaña A, Pandiella A. Resistance to antibody-drug conjugates. Cancer Res 2018;78:2159–65.
17. Helman E, Artieri C, Vowles JV, Yen J, Nance T, Sikora M, et al. Abstract 5603: analytical validation of a comprehensive 500-gene ctDNA panel designed for immuno-oncology and DNA damage research. Cancer Res 2018; 78(Suppl 13):5603.
18. Odegaard JI, Vincent JJ, Mortimer S, Vowles JV, Ulrich BC, Banks KC, et al. Validation of a plasma-based comprehensive cancer genotyping assay utilizing orthogonal tissue- and plasma-based methodologies. Clin Cancer Res 2018;24: 3539–49.
19. Quinn K, Helman E, Nance T, Artieri C, Yen J, Zhao J, et al. Development and analytical validation of a plasma-based tumor mutational burden (TMB) score from next-generation sequencing panels. Ann Oncol 2018;29(Suppl 8):VIII41.
20. Artyomenko A, Sikora M, Lefterova M, Raymond VM, Gavino D, Barbacioru C, et al. Microsatellite instability detection by targeted sequencing of cell-free DNA. Ann Oncol 2018;29(Suppl 8):VIII424.
21. Zheng Z, Liebers M, Zhelyazkova B, Cao Y, Panditi D, Lynch KD, et al. Anchored multiplex PCR for targeted next-generation sequencing. Nat Med 2014; 20:1479–84.
22. Meroni A, Vindigni A. A RADAR method to measure DNA topoisomerase covalent complexes. Methods Enzymol 2022;672:369–81.
23. Urasaki Y, Laco G, Takebayashi Y, Bailly C, Kohlhagen G, Pommier Y. Use of camptothecin-resistant mammalian cell lines to evaluate the role of topoisomerase I in the antiproliferative activity of the indolocarbazole, NB-506, and its topoisomerase I binding site. Cancer Res 2001;61:504–8.
24. Kumar S, Sherman MY. Resistance to TOP-1 inhibitors: good old drugs still can surprise us. Int J Mol Sci 2023;24:7233.
25. Kim N, Jinks-Robertson S. The Top1 paradox: friend and foe of the eukaryotic genome. DNA Repair (Amst) 2017;56:33–41.
26. Arakawa Y, Ozaki K, Okawa Y, Yamada H. Three missense mutations of DNA topoisomerase I in highly camptothecin-resistant colon cancer cell sublines. Oncol Rep 2013;30:1053–8.
27. Mulholland K, Wu C. Computational study of anticancer drug resistance caused by 10 topisomerase I mutations, including 7 camptothecin analogs and lucanthone. J Chem Inf Model 2016;56:1872–83.
28. Sun Y, Chen J, Huang S-YN, Su YP, Wang W, Agama K, et al. PARylation prevents the proteasomal degradation of topoisomerase I DNA-protein crosslinks and induces their deubiquitylation. Nat Commun 2021;12:5010.
29. Pan P, Li Y, Yu H, Sun H, Hou T. Molecular principle of topotecan resistance by topoisomerase I mutations through molecular modeling approaches. J Chem Inf Model 2013;53:997–1006.
30. Yu HA, Baik C, Kim D-W, Johnson ML, Hayashi H, Nishio M, et al. Translational insights and overall survival in the U31402-A-U102 study of patritumab deruxtecan (HER3-DXd) in EGFR-mutated NSCLC. Ann Oncol 2024; 35:437–47.
31. Bansal S, Sur S, Tandon V. Benzimidazoles: selective inhibitors of topoisomerase I with differential modes of action. Biochemistry 2019;58:809–17.